Gravity Investigation of a Recent Crustal Model for Greenland:

Rupert H. Deese
Erik R. Ivins
JPLSIP 2013

Due to extensive ice cover, the geology of Greenland's crust rock is relative mystery. Our understanding primarily comes from global plate tectonic reconstruction and the coastal rock outcrops that provide some ground truth for characterizing the petrology of the crust. Seismic and gravity data, therefore, play relatively prominent roles in determining the physical properties of the crust and mantle-lithosphere, including temperature and heat flow. The thickness, composition, and dynamics of Greenland's crust are important for their effect on Greenland's ice sheet, which is rapidly melting. It is now recognized that our poor understanding of the heat flux from the surface of the crust to the base of the ice sheet critically impacts the numerical simulation of ice sheet dynamics in the face of climate warming, hence severely undermining the veracity of sea-level rise projections into the 22nd Century. Here I attempt to determine the validity of the most recently released (July 20, 2013) global crust model in the region of Greenland by calculating the gravity anomaly due each of the model's layers, and comparing these and their sum, the total crustal anomaly, to the free-air anomaly. The latter is well determined by NASA airborne and satellite missions. I conclude that the model is fundamentally consistent with our current understanding of the lithosphere and asthenosphere of Greenland, but the crust model lacks the spatial resolution necessary to reproduce many of the finer scale features of the observed free air gravity map. Long-wavelength components of the total crustal anomaly support the prediction that the upper mantle beneath continental crust is more dense than the upper mantle beneath oceanic crust. Furthermore, there is good agreement in the magnitude and location of primary short-wavelength components.

I. Introduction

The crustal structure of Greenland beneath the ice sheet cover can best be characterized by employing inversion of geophysical data. Seismic data has been used to make crustal thickness and rock-type estimates [1]; gravity data has also been used to constrain estimates of crustal thickness, employing classical assumptions of isostasy [2]. The new global CRUST1.0 model, constructed dominantly from seismic data, provides crustal thickness and density estimates for

Greenland up to 1x1° resolution [3]. The model is primarily for applying global crust-corrections to seismic wave tomography data. As its resolution increases, it is increasingly used to aid in the seismic monitoring of regional events. The accuracy of the model can be tested by modeling the predicted gravity field, and comparing the prediction to the well-determined free-air gravity anomaly map for Greenland and adjacent environs. A primary motivation for probing Greenland's crust lithosphere environment is to better constraint heat-flux to the base of the ice-sheet. Our current measurement of the latter thermodynamic quantity makes it nearly impossible to generate reliable forecasts of the fate of the ice sheet in a warming climate over the next 100-200 years, and therefore, our ability to predict sea-level rise [4]. The sorts of key features that could so drastically alter our current view of the model heat-flux would be if we were to discover clear evidence for either of late-Cenozoic (younger than about 25 million years) continental rifting or for lithospheric-crustal foundering in the wake of interaction with a mantle hot-spot [5].

A finite element model is created using CRUST1.0 and a new set of bedmap and ice thickness data [6]. The gravitational anomaly due to the model is computed by the gravity field modeling software Tesseroids [7]. Two different approaches are used, one to produce a map of 'total crustal anomaly' for comparison to the free-air anomaly [8], and another following the procedure recently outlined by geodesists to produce a global crust-stripped gravity anomaly map [9].

II. Plate Tectonic Framework

The interpretation of potential field data (gravity and magnetics) is well known for providing geophysicists with a unique but poorly constrained basis for developing models of the Earths interior. However, when seismic information is available and/or when substantial geological information may be brought to bear, gravity data has great power for constraining reasonable models of the Earth's solid interior [10]. The example shown in Figure 1 of free air gravity is from a recent publication by Oakey and Chalmers where a host of geological, ocean floor magnetic and plate tectonic information is used to inform advancements in understanding plate fragmentation in Baffin Bay west of Greenland [11]. In this case the gravity data aided the investigators in sorting out models of sequential ocean spreading and transform faulting events. Coincidentally, one the main fault system being investigated in Figure 1 is the famous "Wegener

Fault", predicted to exist in in the seminal early work on plate tectonic theory by Alfred Wegener [12].

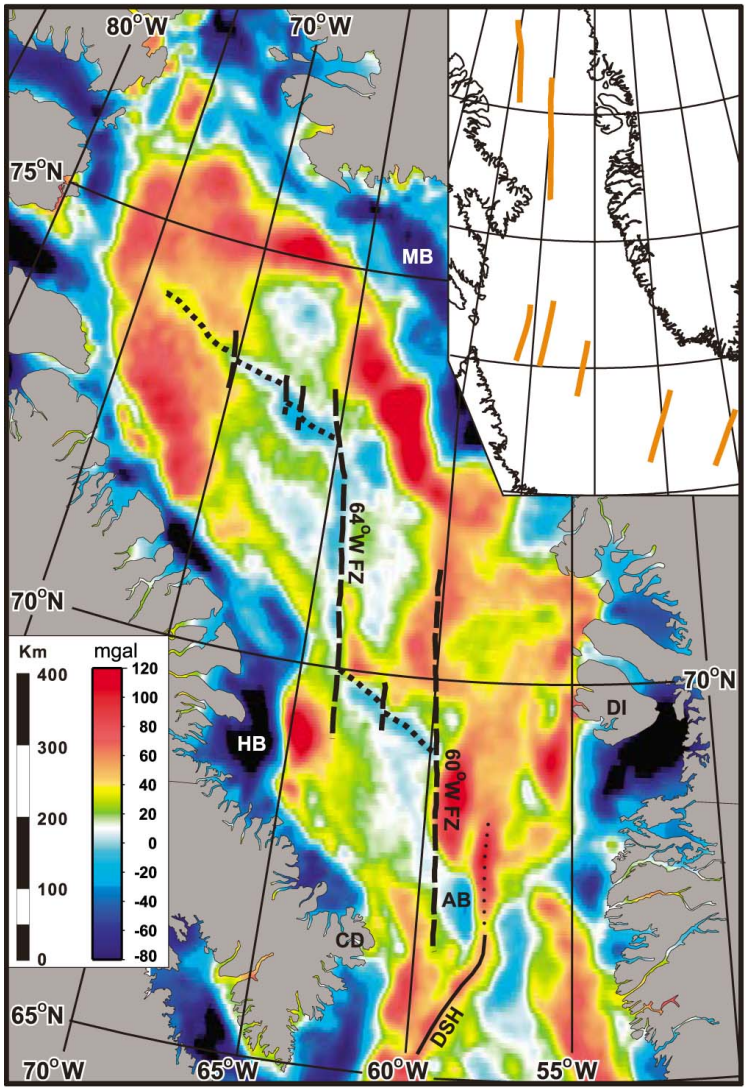

Figure 1. Free air gravity map and extinct ocean crustal spreading axes (dotted lines), major fracture zone (heavy dashed lines) and continental transform margin (or 'strike-slip' fault) in solid line with extinct segment (lightest dashed line). The inset shows lineaments used for plate rotation geometries. From ref. [11].

Similar detailed information exists east of Greenland, and is complicated by the Icelandic Hot Spot, a volcanic complex that has its origins deep in the Earth's mantle as an upwelling plume. The latter influences the crust, lithosphere and mantle of Greenland in unknown ways. One theory is that gravity features in southern and central Greenland reflect the path of the mantle plume that now causes Icelandic volcanism [13, 14]. It is also possible that the free air gravity anomalies in Greenland are related to ancient crust, subsequent suturing of that crust and possibly unrelaxed glacial rebound, such as the negative lows found in Fennoscandia and Hudson Bay.

III. Methods

A. Total Crustal Disturbance

First, CRUST1.0 was globally averaged at depth intervals of 1 km, from the surface down to 60 km, producing a radial density model of the spherical earth (Appendix A).

Second, CRUST1.0 was used to construct a finite-element, spherical-prism model of Greenland's crust (Appendix B). The ice thickness, bed-map, and bathymetry of CRUST1.0 were improved upon by replacing them with new bed-map data assembled by Bamber et al. (Appendix C, D). The prisms composing the model were all 1x1°, with eight prisms stacked vertically at every grid-point, one for each layer.

The *density anomaly* of each prism was calculated by differencing its own density and the density of the earth model at the prism's depth. Choosing an earth model density to use for prisms over 5km thick was problematic, since these spanned a large range of densities in the earth model. To eliminate this problem, every prism in the model was further subdivided vertically, and the density anomaly of each smaller prism was calculated independently. Thus the final model had a 1x1° resolution, and a vertical resolution of 65 prisms (Appendix E).

The gravity anomaly due to the crust model was computed in 8 components, corresponding to the 8 layers of the CRUST1.0 model: water, ice, upper, middle and lower sediments, and upper middle and lower non-sedimentary rock (Appendix F). Tesseroids computes the gravitational attraction of a finite element model of spherical prisms using the formula

$$g_z(r,\phi,\lambda) = G\rho \int_{\lambda_1}^{\lambda_2} \int_{\phi_1}^{\phi_2} \int_{r_1}^{r_2} \frac{\Delta_z}{\ell^3} \kappa dr' d\phi' d\lambda' \quad , \tag{1}$$

where

$$\begin{aligned} \Delta_z &= r' \cos\psi - r \\ \ell &= \sqrt{r'^2 + r^2 - 2r'r\cos\psi} \\ \cos\psi &= \sin\phi \sin\phi' + \cos\phi\cos\phi'\cos(\lambda' - \lambda) \\ \kappa &= r'^2 \cos\phi' \end{aligned} \quad , \tag{2}$$

for the gravitational attraction of each prism. Only the vertical (z) component of the gravitational attraction is calculated, with respect to the local coordinate system of the calculation point. is latitude, is longitude, and *r* is radius. The integral has no analytic solution and is therefore

approximated using a least-squares numerical solution obtained by Gauss-Legendre Quadrature decomposition [15]. Gravitational attraction is measured in milligals (1 mGal = 0.001 cm/s^2).

B. Crust-Stripped Gravity Disturbance

Using the same spherical prism model created in the above procedure, the crust was stripped from the free-air anomaly data in a two-step process. First, the density anomaly of each prism was calculated relative to a reference crust with a density of 2670 g/cm^3. The gravitational attraction of these anomalies was calculated as in the previous procedure, and subtracted from the free-air anomaly data. Then a Tesseroids model of the reference crust was constructed, with no topography, the same depth as the actual crust model, and a density anomaly of -520 g/cm^3. The -520 g/cm^3 value is taken from [9], and represents the anomalous density of the reference crust with respect to an earth model in which the crust is replaced with homogenous mantle at 3190 g/cm^3. The gravitational attraction of this model was also subtracted from the free-air anomaly data, resulting in the crust-stripped gravity anomaly.

IV. Results

According to the CRUST1.0 model, Greenland, Iceland, and the mid-Atlantic ridge are nearly devoid of sediment. In contrast, the surrounding oceanic crust has between 3 and 6 km of ~2000 g/cm^3 sediment. Thicker sediment is found to the northeast and northwest of Greenland. This sediment makes modest contributions to the total crustal anomaly, on the order of ±60 mGal, and generally negative or positive.

Water and ice both make sizable contributions to the total crustal anomaly. The ice contributes a broad, shield-like positive anomaly with a peak of over 100 mGal, while the oceans contribute anomalies exceeding -100 mGal. The topographic correction is not calculated in a single step, but rather split up between the layers that have sections protruding above the surface height.

The upper, middle, and lower non-sedimentary rock layers of the model make the largest contributions to the total crustal anomaly, shown in Figure 2. The oceanic crust, though denser, is much thinner (~10km) than the continental crust (~36km), and the overall effect is a broad negative anomaly over Greenland, trending to positive in the southeast and especially over

Iceland. The result shown in Figure 2 has been corrected for this negative anomaly by a uniform addition of +200 mGal. The contributions of the three layers of oceanic crust are all zero or positive, as is the uppermost layer of non-sedimentary rock over Greenland (~150 mGal average, > 200 mGal over mountains in the east and south). The middle and lower non-sedimentary rock layers contribute negative anomalies (> -100 mGal, > -200 mGal respectively). This is because at depth, the earth model tends towards the density of mantle and exceeds the density of the middle and lower non-sedimentary rocks, resulting in a negative anomalous density.

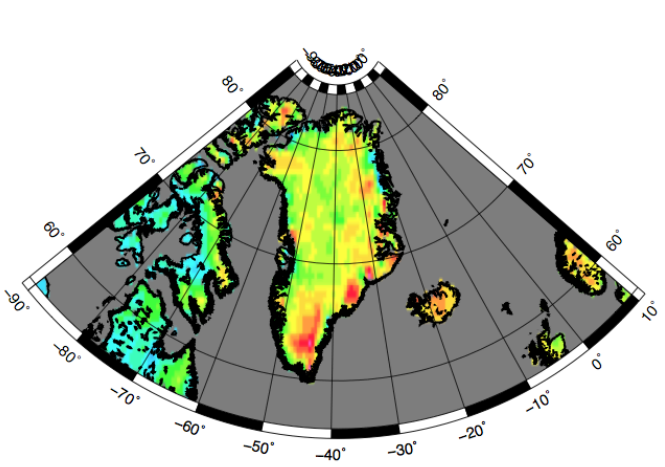

Figure 2. Free-air gravity anomaly over Greenland, compared to the total crustal anomaly calculated using CRUST1.0 and Tesseroids. Both are evaluated at a height of 20km. The total crustal anomaly has been uniformly corrected by +200 mGal to remove the long-wavelength negative anomaly over continental crust.

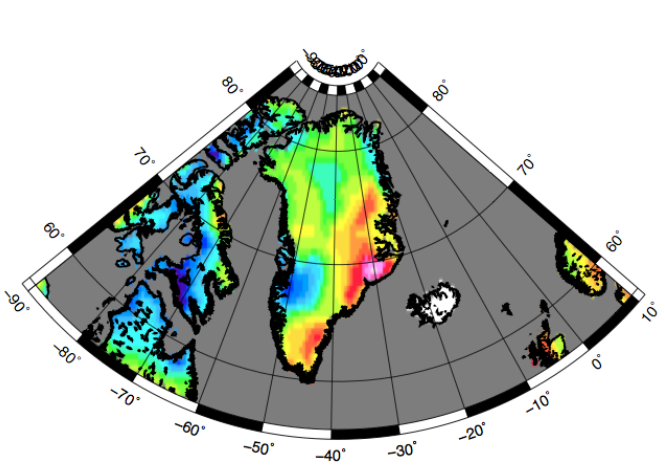

The total crustal anomaly predominately reflects the differences in density and thickness between continental and oceanic crust, as well as the gravity signature of Iceland's mantle plume. With the uniform correction applied, two pronounced lows, one in southwest Greenland and another off

the northeast coast, exceed -100 mGal. Several highs greater than 125 mGal occur along the southeast coast.

Figure 3 shows that the crust-stripped gravity anomaly is similar in both scale and structure to the results found in [9] using the previous iteration of the CRUST model. The crust-stripped gravity anomaly of Greenland (Figure 4) shows a large difference of ~300 mGal between the continental and oceanic upper mantle. This is consistent with the total crustal anomaly, which has an opposite difference of similar magnitude.

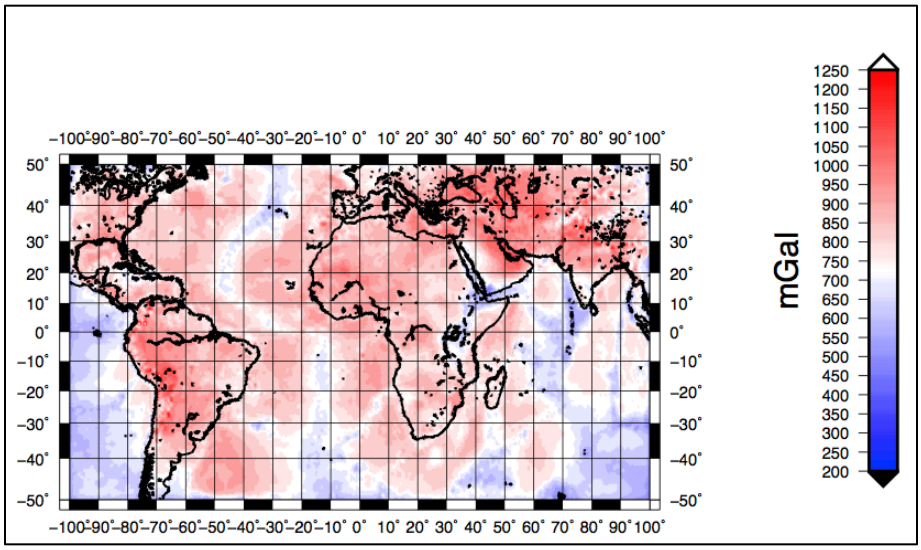

Figure 3. The crust-stripped gravity anomaly over a large section of the earth. The most prominent gravity anomalies reflect density and temperature differences in the upper mantle, which agree with known structure.

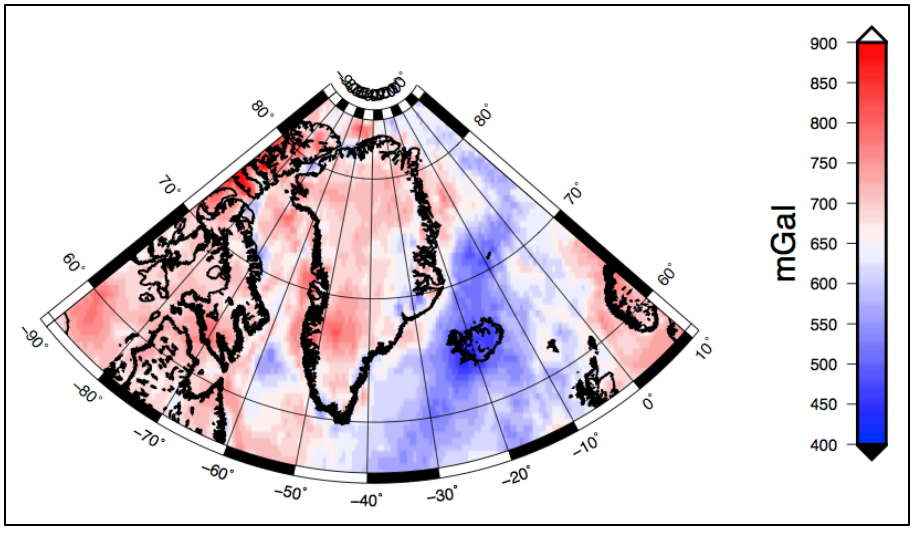

Figure 4. The crust-stripped gravity anomaly over Greenland. The broad negative anomaly in the southeast agrees with the location of the Mid-Atlantic Ridge and Iceland hot spot.

V. Discussion

In contrast to the predictions of the total crustal anomaly, with extremes of ±250 mGal, the observed free air anomaly (see Figure 2, top frame) over Greenland is placid (extremes ±75 mGal). These differences can be explained by shortcomings of the model, isostatic compensation due to density differences extending into upper mantle and below, or some combination of the two. The negative anomaly over Greenland, and the positive anomaly over Iceland and the Mid-Atlantic Ridge can likely be attributed to density differences in the upper mantle: their inversion would give a negative anomaly over the oceanic crust and Mid-Atlantic Ridge, and a positive one over Greenland, reflecting anomalously less dense mantle in the former location, and denser mantle in the latter, a difference that has been observed in the Arctic Ocean [16].

The major short-wavelength gravity anomalies over Greenland all correspond to anomalies visible in the free-air gravity. All originate in the non-sedimentary rock layers of the model. The modeled anomaly in the southwest is caused by thick Proterozoic crust, but is of greater magnitude and much broader than it appears in the free-air gravity. Moho depths in this region are well constrained by seismic data to between 45 and 50km [1]. Rayleigh wave tomography maps show a 2% increase in phase velocity in this area, indicating a relative increase in density [17]. Currently, only the uppermost crustal layer of the model is laterally heterogeneous, which is unrealistic. Since each of the three crustal layers of the model in this region are more than 12 km thick, correcting a relatively small density underestimate in just one of them could vastly reduce the magnitude and extent of the anomaly so that the model better predicts the measured free-air gravity.

The negative anomaly on the northeast coast of Greenland is in the location of the Caledonian fold belt, and coincides with a thickening of the crust that has been previously hypothesized using both seismic and gravity data [18]. At the 1x1° resolution of the model, the extent of the anomaly agrees with the free-air gravity, while the magnitude, as with the anomaly in the southwest, is smaller in the free-air gravity. The free-air gravity resolves an additional vertical division of the anomaly into two distinct lows, which we do not see in the total crustal anomaly. This is probably because the model does not accurately reflect the heterogeneity of the uppermost non-sedimentary rock layer, from which the anomaly originates. The presence of a

band of denser rock in the fold belt would account for the division that is visible in the free-air gravity.

The chain of positive gravity anomalies on the southeastern coast appears in both the total crustal anomaly and the free air anomaly. When the broad, negative continental anomaly in the total crustal anomaly is corrected for, these multiple southeastern coastal anomalies are of approximately the same extent and magnitude. These anomalies come from the upper non-sedimentary rock layer of the model, and correspond strongly to local topography.

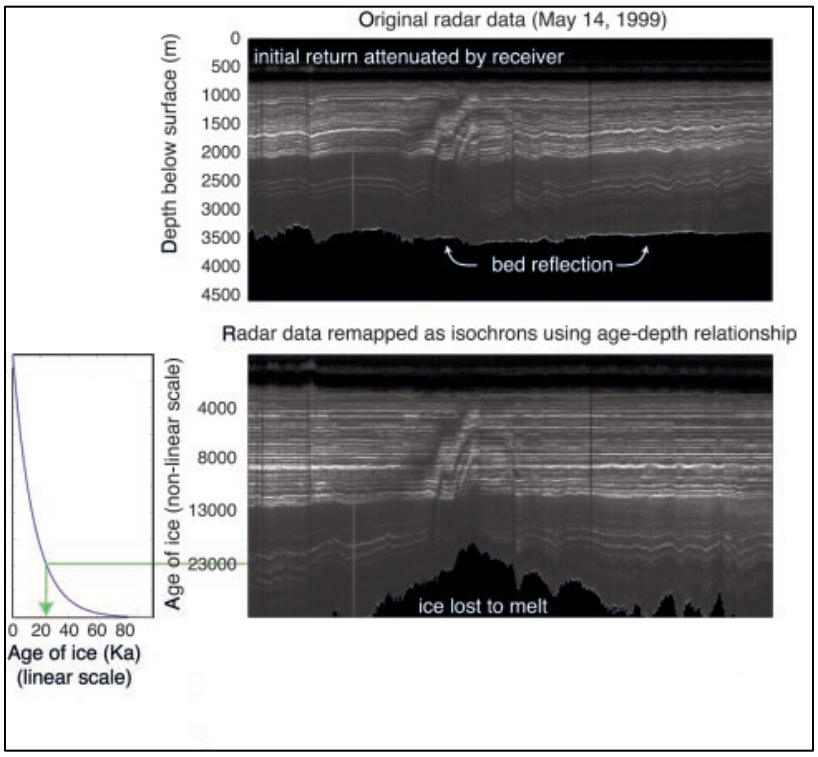

Figure 5. Radar reflection data from the southern limit of the northeast ice stream shows evidence of an extensive melting event 20-25 Ka ago. The x-axis spans 400 km of a NW-SE radar profile, with the northeast ice stream centered at approximately 180 km. From ref. [5].

The resolution of the crustal model is capable of reproducing the main features of the long wavelength components of the free-air gravity. However, there is only marginal, at best, capability to resolve the small anomalies associated with discrete basal heat sources having wavelengths less than 150 km. A caldera hypothesized at the base of the ice sheet is argued to be the source of heat producing the atypical radar reflecting horizons of an ice stream in northeastern Greenland (Figure 5). The crustal and lithospheric features associated with this hypothesis might possibly be appearing in the free-air gravity maps. Unfortunately the new 1x1°

CRUST1.0 model does not have the required resolution for better revealing the structures that would support this hypothesis. A better crustal model is needed before this type of gravity removal can become useful for investigation of basal heat flow and corresponding ice melt. Improvements in crustal models may soon be provided by the newly operating seismic experiments of the Greenland Ice Sheet Monitoring Network (GLISN) (see http://www.glisn.info/).

VI. Appendix: Computational Details

A. A python script (extract-1.py) found the average density at 1km depth intervals between the surface and 60km for the global CRUST1.0 model. The average density was found by averaging the densities of the layer found at a given depth at each grid-point. Where the given depth exceeded the depth of the deepest layer, the mantle density value was used. The radial density model was found, by inspection, to be roughly consistent with the Preliminary Reference Earth Model [19].

B. The CRUST1.0 model provides data in two separate files: a list of layer boundary depths for each grid-point, and a list of layer densities for each grid-point. Lat/lon values were prepended to the data in the Bourne shell, and a Python script (extract-1.py) was used to convert the boundary depths to layer thicknesses, by subtracting the lower boundary from the upper boundary depth for each layer. The script put the data into Tesseroids format: lon, lat, surface elevation, followed pairs of (thickness, density) in depth order starting from the surface. Example: [lon lat sur_elev L1_thick L1_den L2_thick L2_den …]

C. The bedmap, ice, and water layers of CRUST1.0 were replaced by the higher fidelity representations discussed below; the remaining layers were processed by the GMT routines 'blockmean' and 'surface' layer by layer (at 1x1° with -T.25), to ensure the regularity of the data points. Ice thickness, surface elevation, and bedmap from the Bamber dataset were given the same treatment (at 1x1° with -T.25).

D. A Python script (densCalc-1.py) was used to calculate ice and water layer thicknesses from the Bamber data. This was accomplished by assuming that the presence of an ice layer precluded the presence of a water layer. Where ice was present, the ice layer was given a thickness directly from the ice thickness data, and the surface elevation was given to be [bedmap elevation + ice thickness]. Where ice was absent, a water layer was added if the bedmap elevation was less than zero. The water layer was given a thickness such that [bedmap elevation + water thickness] gave a surface elevation of zero. These estimations of surface elevation were compared against the Bamber surface elevation dataset. Differences were shown not to exceed an error threshold of one meter.

   The surface height, ice, and water layers were then welded together, grid-point by grid-

point, to the CRUST1.0 layer data.

E. A Python script was used to generate vertical subdivisions of the model and assign anomalous densities. Each prism was vertically subdivided into 8 prisms of equal height. Additionally, the one of these smaller prisms that spanned the 0km depth was divided into two at that point. The density anomaly for each prism above 0km (above the surface of the spherical earth; negative depth) was just its density. The density anomaly for each prism with a depth greater than 0km was computed by subtracting the radial model's density at the depth of the prism's middle from the prism's density.

F. The Tesseroid script, 'tesslayers', was used to convert the model into Tesseroids format, in which the horizontal and vertical boundaries and density of each prism are explicitly given. With knowledge of how the prisms are organized in the file produced by tesslayers, the UNIX tool 'awk' was used to filter the file and output prisms from only one layer of the model at a time. Layer by layer, the script 'tessgz' was used to calculate the gravity anomaly at points directly over each of the stacks of prisms (that is to say, at each 1x1° grid-point), at a height of 20km.

G. For each layer, the layer's thickness, density (true, not anomalous), and gravity anomaly were plotted on a tri-map using GMT. The gravity anomaly was also 'blockmean' and 'surface' processed to 0.2x0.2° (-T0.25), to optimize visualization of the map renderings. Finally, the Moho depth was calculated by subtracting the total thickness of the layers at each grid-point from that point's surface elevation. The total crustal anomaly was calculated by summing the layer anomalies. These two calculations were plotted, along with the free air anomaly, in a final tri-map.

H. Free air gravity data north of 64° is from ArcGP 2.0. Gravity data south of that is from EGM2008 [20], calculated using the gravity_disturbance_sa function of the ICGEM calculation service [21]. The two datasets agree well and there is no obvious discontinuity between them; thus they were joined without either dataset being manipulated. The data were joined by GMT's grdpaste, and processed by GMT's blockmean and surface (at 1x1° with -T.25).

VIII. Acknowledgements

I am indebted to Erik Ivins for his repeated input, guidance, and scientific insight. I would also like to thank Mathieu Morlighem and Eric Fielding for pointing me in the right direction on separate occasions. I would not have been able to conduct this research without the support of a JPLSIP grant, for which I thank Caltech and JPL, but specifically Carol Casey for all the work she does to make these programs run so smoothly.

VII. Works Cited

[1] Dahl-Jensen, T., Larsen, T. B., et al. (2003), Depth to Moho in Greenland: receiver-function analysis suggests two Proterozoic blocks in Greenland. *Earth and Planetary Science Letters* 205, pp. 379-393.

[2] Braun, A., Kim, H.R., Csatho, B., von Frese, R. (2007), Gravity-inferred crustal thickness of Greenland. *Earth and Planetary Science Letters* 262, pp. 138-158.

[3] Laske, G., Masters., G., Ma, Z. and Pasyanos, M., Update on CRUST1.0 - A 1-degree Global Model of Earth's Crust. *Geophys. Res. Abstracts*, 15, Abstract EGU2013-2658, 2013.

[4] Rogozhina, I., J. M. Hagedoorn, Z. Martinec, K. Fleming, O. Soucek, R. Greve and M. Thomas (2012), Effects of uncertainties in the geothermal heat flux distribution on the Greenland Ice Sheet: An assessment of existing heat flow models, *J. Geophys. Res., 117*, F02025, doi:10.1029/2011JF002098.

[5] Fahnestock, M. et al. (2001), High Geothermal Heat Flow, Basal Melt, and the Origin of Rapid Ice Flow in Central Greenland. *Science* 294, 2338.

[6] Bamber, J. et al. (2013) A new bed elevation dataset for Greenland. *The Cryosphere* 7, pp. 499-510.

[7] Álvarez, O., Gimenez, M., Braitenberg, C. and Folguera, A. (2012), GOCE satellite derived gravity and gravity gradient corrected for topographic effect in the South Central Andes region. *Geophs. J. Int.,* 190, pp. 941–959.

[8] Kenyon, S (2008), New Gravity Field for the Arctic, in *EOS* 89(32), pp. 289-90.

[9] Tenzer, R., Hamayun, K., Vajda, P. (2009), Global maps of the CRUST 2.0 crustal components stripped gravity disturbances. *J. Geophys. Res.*, 114.

[10] Jackson, D.D. (1979) The use Use of a priori data to resolve non-nniqueness in iinear inversion, *Geophys. J. R. Astr. Soc., 57*, 137-157.

[11] Oakey, G. N., and J. A. Chalmers (2012), A new model for the Paleogene motion of Greenland relative to North America: Plate reconstructions of the Davis Strait and Nares Strait regions between Canada and Greenland, *J. Geophys. Res., 117*, B10401, doi: 10.1029/2011JB008942.

[12] Wegener, A., (1912). Die Entstehung der Kontinente, *Geologische Rundschau* (in German), *3* (4), 276–292.

[13] Mihalffy, P., B. Steinberger, H. Schmeling, (2008), The effect of the large-scale mantle flow field on the Iceland hotspot track, *Tectonophysics, 447*, 5-18.

[14] Kumar, P., R. Kind, W. Hanka and 12 others, (2005). The lithosphere–asthenosphere boundary in the North-West Atlantic region, *Earth Planet. Sci. Lett., 236*, 249-257.

[15] Asgharzadeh, M. F., R. R. B. von Frese, H. R. Kim, T. E. Leftwich, and J. W. Kim (2007), Spherical prism gravity effects by Gauss-Legendre quadrature integration, Geophysical Journal International, 169(1), 1-11.

[16] Krysinski, L., Grad, M., Mjelde, R., Czuba, W., Guterch, A. (2013), Seismic and density structure of the lithosphere–asthenosphere system along transect Knipovich Ridge –Spitsbergen–Barents Sea – geological and petrophysical implications. *Polish Polar Research,* 34(2), pp. 111-138.

[17] Darbyshire, F. A., et al. (2004), A first detailed look at the Greenland lithosphere and upper mantle using Rayleigh wave tomography. *Geophys. J. Int.,* 158, pp. 267-286.

[18] Schmidt-Aursch, M. C., Jokat, W. (2005), The crustal structure of central East Greenland—II: From the Precambrian shield to the recent mid-oceanic ridges, *Geophys. J. Int.*, 160(2), pp. 753-760.
[19] A. M. Dziewonski, D. L. Anderson (1981), Preliminary reference Earth model. *Phys. Earth Planet. Inter.* 25, 297.
[20] Pavlis, N. K., S. A. Holmes, S. C. Kenyon, and J. K. Factor (2012), The development and evaluation of the Earth Gravitational Model 2008 (EGM2008). *J. Geophys. Res.*, 117, B04406.
[21] Barthelmes, F. (2009), Definition of Functionals of the Geopotential and Their Calculation from Spherical Harmonic Models. *Deutsches Geo- Forschungs Zentrum GFZ.*